

XAFS studies of gold and silver-gold nanoparticles in aqueous solutions

Tomohiro Shibata,^{a,*} Holger Tostmann,^b
Bruce Bunker,^a Arnim Henglein,^c Dan Meisel,^c
Seongkyun Cheong^a and Maxim Boyanov^a

^aDepartment of Physics, University of Notre Dame, Notre Dame IN 46556, USA, ^bDepartment of Chemistry, University of Florida, Gainesville, FL 32611, USA, and ^cDepartment of Chemistry and Radiation Laboratory, University of Notre Dame, Notre Dame IN 46556, USA. E-mail: tshibata@darwin.helios.nd.edu

The x-ray absorption fine structure (XAFS) of colloidal Au and Au/Ag nanoparticles (3.5nm and 20nm mean diameter) in an aqueous solution has been investigated. Size dependent alloying was observed upon deposition of Ag on Au core. Ag forms distinct layers around the 20 nm Au nanoparticles. In contrast, random mixing is found for Ag deposited on 3.5nm Au particles.

Keywords: nanoparticles, XAFS, alloy, gold, silver.

1. Introduction

Metallic nanoparticles in solution have recently gained great interest because of their catalytic (Haruta, 1997, Grunwaldt *et al.*, 1999) and electronic properties (Henglein, 1993; Link & El-Sayed, 1999). The structure of these particles can be investigated by high-resolution transmission electron microscopy (TEM); however, this technique yields no information about the internal structure of nano-composites. Most previous XAFS studies on nanoparticles were performed on particles on solid support. Here we report an XAFS study of nanoparticles suspended in solution. Both, single metal (Au) and core-shell particles (Ag shell on Au core) were studied.

2. Experimental

20nm diameter gold particles of a narrow size distribution (10% standard deviation) were prepared by reducing AuCl_4^- by citrate (Henglein & Meisel, 1998), and 3.5nm diameter particles with a wider size distribution ($\pm 0.5\text{nm}$) via radiolytic reduction of AuCl_4^- . Particles size, morphology, and the size distribution were determined by TEM as described previously (Henglein, 1999). The Ag layer was deposited by adding the desired amount of $\text{Ag}(\text{CN})_2^-$ to the colloidal Au and reducing the Ag complex radiolytically on the surface of the Au particles (Hodak *et al.*, 2000). 1-6 atomic Ag layers were deposited on the 20nm Au particles, and one monolayer on the 3.5nm particles. In order to prevent the nanoparticles from coagulating, the outermost atomic layer necessarily carries some charged species (mostly citrate in this case). However, no effect of the ligand coverage on the XAFS spectra was observed. The concentration of metal particles typically varies around $5 \times 10^{-4}\text{M}$.

These solutions were investigated by fluorescence XAFS at the Au L_3 edge using a conventional Lytle detector at room temperature. Because of the low concentration of the sample, we used a thick x-ray filter (nine absorption lengths at the Au edge) and Soller slits to reduce the scattered background. Because of artifacts from radiolysis bubbles, several scans were taken, changing the liquid or

sample positions and the spectra were averaged. All the measurements were performed at the MRCAT undulator beamline at the Advanced Photon Source. Data analysis was done using FEFFIT (Newville, *et al.*, 1995) and FEFF6.01.(Rehr *et al.*, 1992).

3. Results and Discussion

We measured a Au foil standard as well as pure Au nanoparticles of 20nm and 3.5nm. The Au-Au nearest neighbor distance as obtained from fitting the Au foil data is about 0.02\AA shorter than the bulk crystallographic bond length using XAFS scattering calculations from FEFF6.01. This well-known effect is due to the fact that the near-neighbor Au-Au distribution is slightly asymmetric at room temperature for Au. In this paper, we analyzed the data without including the higher cumulants, instead showing changes in bond length relative to that of the bulk. This is justified as the Debye Waller factor (DWF) observed for these nanoparticles is very close to that of the bulk, showing a similar degree of disorder. Relative to the distance in the Au foil, the Au-Au nearest neighbor distance is shorter by $0.026 \pm 0.01\text{\AA}$ in the 3.5nm Au nanoparticles. On the other hand, the Au-Au bond lengths are about the same in the 20nm pure Au nanoparticles and the Au foil, consistent with previous XAFS measurements (Balerna *et al.*, 1985). The data for the pure 3.5nm Au particles can be fitted with a coordination number (CN) of 10.6 ± 1.2 and the DWF of $(9 \pm 1) \times 10^{-3}\text{\AA}^2$; this is a reasonable reduction of the CN considering the increased number of surface atoms relative to fully coordinated core atoms.

XAFS spectra of Au nanoparticles of 20nm diameter with different degrees of deposition of Ag (molar ratios Au:Ag of (a) 8:1 (b) 4:1 (c) 2:1) were measured. This corresponds to 1.7, 3.3, and 6.2 atomic layers of Ag on a Au core respectively for (a), (b), and (c), assuming that no alloy formation takes place in the core. The XAFS spectra of (a) - (c) look similar to those of the pure Au nanoparticles, indicating that Ag forms layers around the Au core without affecting it. We analyzed the first shell data only even though higher shell features are discernible. To describe the first shell of the 20nm Au/Ag nanoparticles, six parameters have to be determined: the CN, the bond length and the DWF for both the Au-Au and the Au-Ag pairs. However, due to the limited data range, the number of degrees of freedom is limited and not all the parameters can be varied at once. Since the majority of the Au-Au pairs are located in the Au core and the core is essentially unaffected by the Ag deposition, it is reasonable to assume that the bond length and the DWF for the Au-Au pairs are the same for the pure 20nm Au particles and the 20nm Au particles with Ag added. This leaves us with the CN, the bond length and the DWF for the Au-Ag pairs, as well as the CN of Au-Au pairs as variables. This assumption is consistent with the fitting results shown below.

Table 1 shows the fitting results for Au/Ag colloids. N_{tot} is the total CN of the nearest neighbors of the Au, $N_{\text{tot}} = N(\text{Au}) + N(\text{Ag})$; $N(\text{Au})$ and $N(\text{Ag})$ are the CN of Au and Ag around Au; $N(\text{Ag})/N_{\text{tot}}$ is the ratio of Ag to the total number of neighbors around Au; $\Delta R_{\text{Au-Au}}^{\text{Nano}}$ and $\Delta R_{\text{Au-Ag}}^{\text{Nano}}$ are the changes in bond lengths for Au-Au ($R_{\text{Au-Au}}^{\text{Nano}}$) and Au-Ag ($R_{\text{Au-Ag}}^{\text{Nano}}$) relative to that of bulk Au-Au ($R_{\text{Au-Au}}^{\text{Bulk}}$), defined as $\Delta R_{\text{Au-Au}}^{\text{Nano}} = R_{\text{Au-Au}}^{\text{Nano}} - R_{\text{Au-Au}}^{\text{Bulk}}$ and $\Delta R_{\text{Au-Ag}}^{\text{Nano}} = R_{\text{Au-Ag}}^{\text{Nano}} - R_{\text{Au-Au}}^{\text{Bulk}}$ respectively. The DWF for the Au-Ag bond is $(9 \pm 1) \times 10^{-3}\text{\AA}^2$ for (a) - (c). In the series of (a) - (c), a small portion of Ag atoms ($N(\text{Ag})/N_{\text{tot}}$) is observed in the first shell around Au with little sample dependence. The uncertainty is somewhat large, because of parameter correlation, but for all of these samples $N(\text{Ag})/N_{\text{tot}}$ is less than 9 % assuming the maximum possible error

Table 1

XAFS parameters for pure Au and Au/Ag nanoparticles. (a), (b), and (c) are Au(20nm)/Ag nanoparticles with Au:Ag=8:1, 4:1, and 2:1 respectively, and (d) is Au(3.5nm)/Ag with Au:Ag=2:1. N_{tot} is the sum of coordination numbers of Au and Ag around Au, and $N(Ag)/N_{tot}$ is the contribution of the Ag neighbors to the Au XAFS scattering path. ΔR_{Au-Au}^{Nano} and ΔR_{Au-Ag}^{Nano} are the difference in bond length of Au-Au (R_{Au-Au}^{Nano}) and Au-Ag (R_{Au-Ag}^{Nano}) for nanoparticles relative to the fitting value for the bulk (R_{Au-Au}^{Bulk}) defined as $\Delta R_{Au-Au}^{Nano} = R_{Au-Au}^{Nano} - R_{Au-Au}^{Bulk}$ and $\Delta R_{Au-Ag}^{Nano} = R_{Au-Ag}^{Nano} - R_{Au-Ag}^{Bulk}$ respectively and given in Å. The large error bar in ΔR_{Au-Ag}^{Nano} for (a)-(c) is due to the small effect of Ag on the Au XAFS.

Sample	N_{tot}	$N(Ag)/N_{tot}$	ΔR_{Au-Au}^{Nano}	ΔR_{Au-Ag}^{Nano}
Au _{foil}	12 (fix)	0	0 (fix)	–
Au _{20nm}	11.5±1.0	0	-0.01±0.01	–
Au _{3.5nm}	10.6±1.2	0	-0.026±0.01	–
a	11.5±1.2	0.04±0.04	-0.01(fix)	0.06±0.08
b	11.5±1.2	0.03±0.03	-0.01(fix)	0.02±0.07
c	12.4±1.2	0.06±0.03	-0.01(fix)	-0.02±0.04
d	11.6±0.7	0.27±0.05	-0.03±0.01	-0.02±0.02

bar.

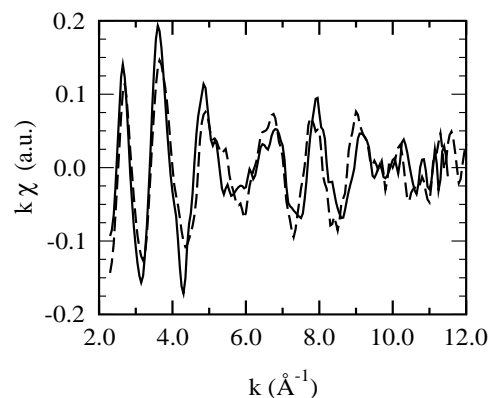
Based on the values given in Table 1, we consider the following models for the internal structure of the Au/Ag nanoparticles with a 20nm Au core: The TEM image shows that the particles are spherical and the size distribution is reasonably uniform (Henglein, 1999). This greatly facilitates the interpretation of XAFS data which average over all particles. First, we consider the formation of Ag layers on the Au core. For simplicity, we assume an FCC (111) lattice on the surface and for the outermost Au atoms, 3 out of the 12 nearest neighbors are replaced by Ag. About 7% of the Au atoms are facing the surface in the case of 20nm Au particles, so only an average 2% contribution of the Ag atoms should be observed independent of the amount of Ag deposition. This is consistent with our experimental finding that the Ag essentially does not affect the Au data. Next we consider complete miscibility within the particle as a whole. This model gives the contribution of Au-Ag scattering of 11, 20, and 33 % respectively for (a), (b), and (c), thus a completely random distribution of Ag within the particle is well outside the experimental error for all three samples (a) - (c). We cannot rule out that some of the Ag alloys with the Au core but at least one complete layer of Ag at the outermost surface layer of the particle has to be assumed in order to explain the data for sample (c).

Now we discuss the sample (d), which is a 3.5nm Au core with Ag added. The amount of Ag is Au:Ag=2:1, which is about one atomic monolayer on the surface of the Au core. Fig.1 shows a distinct difference especially in the phase of the XAFS oscillation for the pure 3.5nm Au particles compared to the 3.5nm Au nanoparticles with Ag added. Fortunately, large differences in the backscattering phase and amplitude for Au-Au and Au-Ag pairs allow for the discrimination between a heterogeneous particle – where the Au is only slightly affected by the presence of Ag layers at the outermost layers – and a random alloy particle – where the Au is surrounded by a significant number of Ag atoms. This feature appears as the double peak in the real space data in Fig.2. The two peaks around 2.4Å and 3.0Å are the first shell data split due to the dip in the backscattering amplitude vs. k for Au. Here we see that the relative intensity of the double peak is markedly changed with Ag deposition. We find that $N(Ag)/N_{tot}$ is $27\pm 5\%$. In the fitting, the bond length and the DWF for the Au-Au pair are also left as fitting variables, in addition to those used for the 20nm Au/Ag nanoparticles in spite of parameter correlation. We comment that

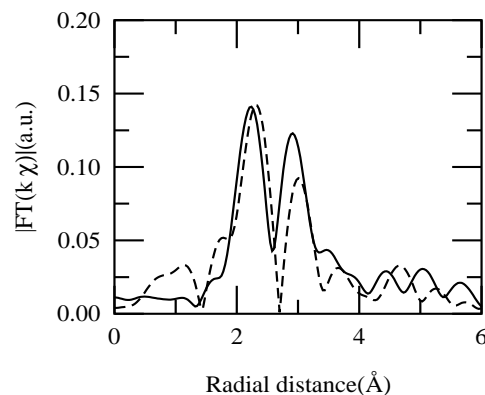
the $N(Ag)/N_{tot}$ has smaller correlation with the DWF than N_{tot} as long as the DWF of Au-Au and Au-Ag pair have a similar value.

Again, we compare our data to the two possible models: First we consider the case of a heterogeneous particle with Ag forming layers around the Au core. Since the 3.5nm particles have about 40% of the Au particles facing the surface, $N(Ag)/N_{tot}$ should be 10%, which is not consistent with the experimental data. Next we consider homogeneous alloying of Au with Ag within the particle: Random alloy formation would result in Ag being 33% of the atoms in the Au nearest neighbor coordination shell, which is consistent with our data. The smaller reduction of N_{tot} for Au/Ag nanoparticles compared with 3.5nm Au nanoparticles can be understood if we consider that only $\sim 67\%$ of the surface atoms are Au when a random alloy is formed.

It is important to discuss the effect of the size distribution on the analysis of our data since the 3.5nm particles have a wider size distribution function than the 20nm particles. For a nanoparticle, the ratio of the surface atoms to the inner atoms increases when the size becomes smaller. However, the number of atoms in the particles decreases more rapidly. Therefore, the average ratio of the surface atoms to the inner atoms is mainly determined by the number distribution of the larger particles. Since the distribution obtained


Figure 1

$k\chi$ of 3.5nm Au nanoparticles (dotted line) and Au(3.5nm)/Ag nanoparticles with Ag (Au:Ag=2:1) (sample (d)).


Figure 2

Amplitude of Fourier transform of Au nanoparticles(3.5nm) (dotted line) and Au(3.5nm)/Ag nanoparticles (Au:Ag=2:1) (sample (d)) (solid line).

from the TEM image is nearly symmetric, the distribution effect reduces the number of the surface atoms. It should also be stressed that the growth of the radius of the particle is faster for smaller particles and the ratio of Ag/Au deposited should be larger for a smaller Au core. Both of these effects indicate a layered structure would result in less than 10% backscattering from Ag which is clearly inconsistent with our data for 3.5nm nanoparticles. This striking size dependence is under investigation, with studies of a number of different particle sizes and compositions planned.

4. Summary and Conclusions

We successfully measured nano-sized Au and Au/Ag colloidal nanoparticles in a dilute solution using XAFS to study the internal structure of ligand- and support-free nanoparticles. By comparing Ag deposition on differently sized Au cores we conclude:

(i) when Ag is deposited on a 20nm Au core, Ag and Au form an interface with at most several layers of interdiffusion. The data are inconsistent with the formation of a homogeneous Au/Ag alloy.

(ii) when Ag is deposited on a 3.5nm core, Au and Ag form a homogeneous alloy and the data are inconsistent with the layer formation found for the larger nanoparticles.

This striking difference is reproducible and is apparently a size effect. Further studies of the nanocomposites, varying the particle

size, composition, and preparation methods are underway.

This work is supported by the Office of Basic Energy Science of the US Department of Energy (DOE) as contribution NDRL 4262 of the Notre Dame Radiation Laboratory. The MRCAT is supported by the DOE under Contract DE-FG02-94-ER45525 and the member institutions. The Advanced Photon Source is supported by the DOE, under Contract No.W-31-102-Eng-38.

References

- Balerna, A. Bernieri, E. Picozzi, P. Reale, A. Santucci, S. Burattini, E. & Mobilio, S. (1985) *Phys.Rev.B.* **31**, 5058–5065.
- Grunwaldt, J.D. Kiener, C. Wogerbauer, C. & Baiker, A. (1999). *J.Catal.* **181**, 223–232.
- Haruta, M. (1997). *Catal.Today* **36**,153–166.
- Henglein, A. (1993). *J.Phys.Chem.* **97**,5457–5471.
- Henglein, A. & Meisel, D. (1998). *Langmuir* **14**,7392–7396.
- Henglein, A. (1999). *Langmuir* **15**,6738–6744.
- Hodak, J.H. Henglein, A. Giersig, M. & Hartland, G.V. (2000). *J.Phys.Chem. B* **112**,5942–5947.
- Link, S & El-Sayed, M.A. (1999). *J.Phys.Chem.B.* **103**,8410–8426.
- Mulvaney, P. Giersig, M. & Henglein, A. (1993). *J.Phys.Chem.* **97**,7061–7064.
- Newville, M. Ravel, B. Haskel, D. Stern, E. & Yacoby, Y. (1995). *Physica B* **208&209**, 154–156.
- Rehr, J. Albers, R.C. & Zabinski, S. (1992). *Phys.Rev.Lett.* **69**,3397–3400.